Proc. Natl. Acad. Sci. USA
Vol. 79, pp. 3125–3128, May 1982
Biochemistry

Gross quaternary changes in aspartate carbamoyltransferase are induced by the binding of *N*-(phosphonacetyl)-L-aspartate: A 3.5-Å resolution study

(protein crystallography/enzyme activation)

J. E. LADNER, J. P. KITCHELL, R. B. HONZATKO, H. M. KE, K. W. VOLZ, A. J. KALB (GILBOA)†, R. C. LADNER, AND W. N. LIPSCOMB

Gibbs Chemical Laboratory, Harvard University, 12 Oxford Street, Cambridge, Massachusetts 02138

Contributed by W. N. Lipscomb, February 11, 1982

ABSTRACT **The three-dimensional structure of the complex of *N*-(phosphonacetyl)-L-aspartate with aspartate carbamoyltransferase (carbamoylphosphate:L-aspartate carbamoyltransferase, EC 2.1.3.2) has been determined to a nominal resolution of 3.5 Å by single-crystal x-ray diffraction methods. Initial phases were obtained by the method of "molecular tectonics": beginning with the structure of the CTP–protein complex, the domains of the catalytic and regulatory chains were manipulated as separate rigid bodies. The resulting coordinates were used to calculate an electron density map, which was then back transformed to give a set of calculated amplitudes and phases. Using all observed data, we obtained a crystallographic *R* factor between observed and calculated amplitudes F_o and F_c of 0.46. An envelope was then applied to a $2F_o - F_c$ map and the density was averaged across the molecular twofold axis. Two cycles of averaging yielded an *R* factor of 0.25. In this complex, we find that the two catalytic trimers have separated from each other along the threefold axis by 11–12 Å and have rotated in opposing directions around the threefold axis such that the total relative reorientation is 8–9°. This rotation places the trimers in a more nearly eclipsed configuration. In addition, two domains in a single catalytic chain have changed slightly their spatial relationship to each other. Finally, the two chains of one regulatory dimer have rotated 14–15° around the twofold axis, and the Zn domains have separated from each other by 4 Å along the threefold axis. These movements enlarge the central cavity of the molecule and allow increased accessibility to this cavity through the six channels from the exterior surface of the enzyme.**

Aspartate carbamoyltransferase (carbamoylphosphate:L-aspartate carbamoyltransferase, EC 2.1.3.2) from *Escherichia coli* catalyzes the formation of carbamoyl-L-aspartate from L-aspartate and carbamoylphosphate. This reaction is the first committed step in pyrimidine biosynthesis in many prokaryotes. The enzyme is regulated homotropically by sigmoidal dependence on the concentration of both substrates (1, 2). It is also regulated heterotropically; the presence of CTP, the product of the triphosphate pyrimidine pathway, causes inhibition (3), whereas ATP, a product of the complementary purine pathway, causes activation (1). Such extensive regulation suggests complex ligand-induced conformational changes. The simplest model postulates two quaternary enzyme conformations: the inactive T (tense) state and the active R (relaxed) state (4).

Aspartate carbamoyltransferase is composed of two catalytic chain trimers (c_3) and three regulatory chain dimers (r_2) (5–7). A pair of schematic drawings of the enzyme, showing the one threefold and three twofold axes, is shown in Fig. 1. The structure of the T state of the enzyme is known (7) and has been refined at 2.8-Å resolution (8).

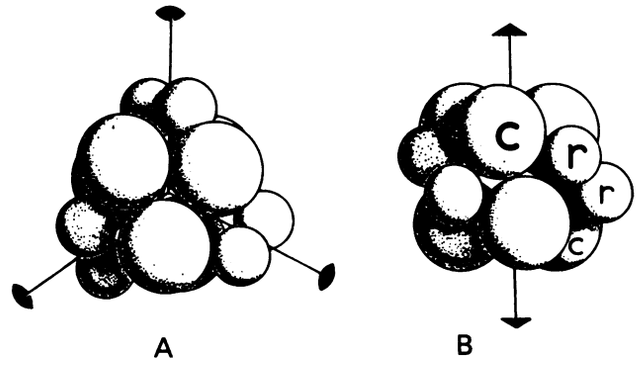

FIG. 1. Schematic drawings of the aspartate carbamoyltransferase molecule. (*A*) View down the threefold axis showing one c_3 (large spheres), three r_2s (small spheres), and the three twofold axes. (*B*) View along a twofold axis perpendicular to the threefold axis with a c–r–r–c unit marked.

Many lines of evidence (recently reviewed in refs. 9 and 10) suggest that conversion to the R state involves very large conformational changes. Studies in solution have demonstrated that the gross structural changes that occur during the substrate activation of the enzyme also occur in the presence of *N*-(phosphonacetyl)-L-aspartate (PALA) (11, 12), which is a potent reversible inhibitor of aspartate carbamoyltransferase (11). This compound is an unreactive bisubstrate analogue that has a methylene group replacing the mixed-anhydride oxygen of carbamoylphosphate. The chemical, spectroscopic, and crystallographic evidence for gross conformational changes induced in the enzyme structure by PALA led us to search for these changes by solving the crystal structure of the complex.

MATERIALS AND METHODS

Crystal Growth. Mutant *E. coli* (provided by J. C. Gerhart) were grown at the New England Enzyme Center. Aspartate carbamoyltransferase was isolated by the method of Gerhart and Holoubek (13). The enzyme was stored at −20°C as an 18 mg/ml solution in 1:1 (vol/vol) glycerol/storage buffer (40 mM K_2PO_4/2.0 mM 2-mercaptoethanol/0.2 mM EDTA, pH 7.0). Before use, the protein solution was passed through a 0.45-μm-

The publication costs of this article were defrayed in part by page charge payment. This article must therefore be hereby marked "*advertisement*" in accordance with 18 U. S. C. §1734 solely to indicate this fact.

Abbreviations: PALA, *N*-(phosphonacetyl)-L-aspartate; c, catalytic subunit; r, regulatory subunit.

† Present address: Dept. of Biophysics, Weizmann Institute, Rehovot, Israel 76100.

pore-diameter Millipore filter and dialyzed overnight at 4°C against storage buffer (6 ml of protein solution per 1 liter of buffer).

The protein in storage buffer (10–18 mg/ml) was placed in bags made from Spectrapor semimicro dialysis tubing of 4-mm width (obtained from Fisher). Into each bag we added 0.2–1.0 ml of protein solution. Bags were then placed in 10 ml of crystallizing buffer (50 mM maleic acid/1.0 mM PALA/0.003 mM NaN_3/*N*-ethylmorpholine to pH 5.8) and left undisturbed for 4 days at room temperature. We prepared the $K_2Pt(NO_2)_4$ derivative by immersing a crystal of the PALA-inhibited enzyme in soaking buffer [50 mM Tris/maleic acid, pH 5.8 with NaOH/1 mM PALA/12% (vol/vol) polyethylene glycol 6,000/0.5 mM $K_2Pt(NO_2)_4$].

Data Collection and Analysis. Crystals of the PALA–aspartate carbamoyltransferase complex in the space group *P*321 are hexagonal prisms that have unit cell dimensions of $a = b = 122$ Å and $c = 155$ Å. Typically, we used crystals that were 1.5–2.0 mm long and 0.5–1.2 mm wide. Only one or two crystals were needed for a complete set of data. These data were collected on an Elliot GX6 rotating anode at 39 kV and 19 mA, with the use of a 100-μm focusing cup. Each oscillation photograph was taken over a 1° interval, and either the c^* or a^* axis was oriented coaxially with the spindle. The resulting films were scanned on an Optronics p1000 Photoscan interfaced with a PDP 11/20 computer (Digital Equipment), using software developed by Crawford (14). Computations were done on a VAX 11/780 computer (Digital Equipment). We used the rotation-function program of Crowther (15, 16) as follows: for 6- to 8-Å resolution data Patterson vectors up to 35 Å were included, and for 4- to 6-Å data, the Patterson vector cutoff was 25 Å. In order to obtain the forward and reverse transforms of the maps, the fast Fourier transform package of Ten Eyke (17, 18) was employed. The noncrystallographic averaging method of Bricogne (19, 20) was used to perform the molecular twofold averaging. For this purpose, we recently developed a program that allows us to create the envelope on an Evans and Sutherland multi-picture system. A $2F_o - F_c$ map, calculated on a 1-Å grid, was averaged using data to 4 Å in the first cycle and all the data in the second cycle (F_o, observed amplitudes; F_c, calculated amplitudes).

RESULTS AND DISCUSSION

Crystals of the PALA–aspartate carbamoyltransferase complex have been characterized in three different space groups (21, 22). From a data set taken to 3.5 Å in the space group *R*32 ($a = b = 122$ Å, $c = 706$ Å), the reflections to 5.5 Å were used in a molecular replacement study in which only a relative twist of the c_3s was noted (23). Study of this crystal form is not yet complete. We chose the crystals of *P*321 symmetry for the present study because of their comparatively manageable unit cell dimensions, and because of their close relationship to the crystal form of the CTP–enzyme complex. A lengthy search for a reliable method of obtaining this form was concluded with the simultaneous development of two methods. First, CTP–enzyme *P*321 crystals were converted to the unit cell of the PALA *P*321 form (slightly longer along the *c* direction) after soaking in a citrate/phosphate buffer. Alternatively, the *P*321 PALA–aspartate carbamoyltransferase crystals grew rapidly and reproducibly as described in *Materials and Methods*. These latter crystals were used for data collection.

The two molecules in the unit cell of the *P*321 crystals lie on the threefold axes, (2/3, 1/3, ≈1/4) and (1/3, 2/3, ≈3/4), and are related by a twofold crystallographic axis. The isolated molecule has three twofold axes perpendicular to the threefold axis. We have established by the self-rotation of both the native data and the Pt heavy atom differences that the angle between each

Table 1. Intramolecular parameters in the molecular tectonics model

	c (polar)	c (equatorial)	r (nucleotide-binding)	r (Zn)
Residues	(1–140, 285–end)	(141–284)	(1–100)	(101–end)
Threefold rotation, °	4	5	0	0
Twofold rotation, °	0	−1.5	14	15
Δx, Å	0	2	0	−1
Δy, Å	0	0	0	0
Δz, Å	6.0	5.5	0	2.0

The directions of the rotations can be seen in Fig. 2. The movements in *x*, *y*, and *z* refer to an orthogonal system in which *z* is coincident with the threefold axis and *y* is coincident with a twofold axis. The change in *x* is toward the twofold axis for the c domain and away from the twofold axis for the r domain. The changes in *z* are increases in the distances away from the molecular center.

of these molecular twofold axes and the nearest crystallographic twofold axis is 12°. This orientation is 4.5° away from the molecular twofold axis in the CTP–enzyme crystals.

Phases from heavy atom derivatives have not yielded an interpretable electron density map. We have collected data sets from several derivatives that have multiple low occupancy sites. All of these derivatives require further analysis.

The location of a Pt site from a difference Patterson map provided an important clue in determining the extensive changes in quaternary structure that we were to encounter. This site had the same *x*, *y* coordinates as a site that had been reported in the c_3 of the CTP–enzyme complex. This result seemed curious to us because, as mentioned above, from the locations of the two-

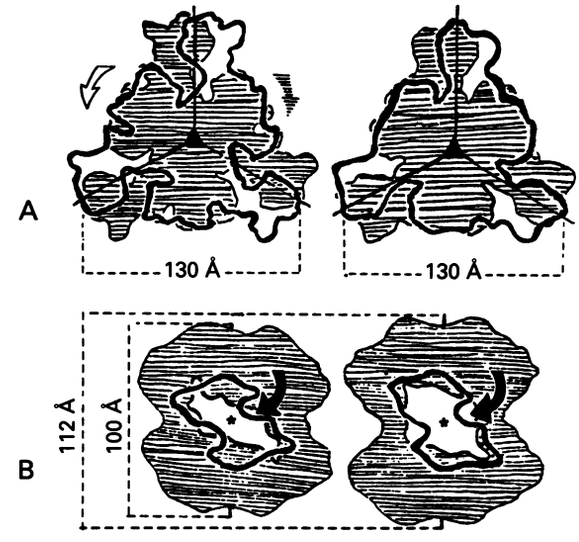

FIG. 2. Changes in relative positions of the subunits. (*A*) View down the molecular threefold axis. The lower c_3 and the three lower rs are represented by the shaded area. The upper c_3 and the three upper rs are represented by the heavily outlined area. The CTP–enzyme complex is on the left, the PALA–enzyme complex is on the right. The directions of c_3 rotation that accompany conversion from T to R state are indicated by the open arrow for the upper c_3 and the shaded arrow for the lower c_3. (*B*) View down the molecular twofold axis. Four c chains, those closest to the viewer, are represented by the shaded area. One r_2 is represented by the heavily outlined area. The open space is the central cavity. The access to the cavity, which is unobstructed from this viewpoint, is marked with an arrow. The CTP–enzyme complex is on the left, the PALA–enzyme complex is on the right. The access to the central cavity is enlarged in the R state.

fold axes we knew that the crystallographic orientation of the PALA–enzyme molecule was different from that of the CTP complex. The explanation is that the intramolecular twisting of the c_3s around the threefold axis is 9° relative to each other in the PALA complex. Thus, the two c_3s each move 4.5° about the molecular threefold axis, but in opposite directions. Coincidentally, this rotation is just the difference in orientation of the molecular twofold axes positions between the two forms. Therefore, one c_3 remains in the same position in both the CTP and PALA complex crystals, while the other is reoriented by 9°.

Using the CTP–enzyme structure, modified as described above, we attempted to solve the PALA–enzyme structure by the method of molecular replacement. However, the resulting three-dimensional electron density did not reveal discernible molecular boundaries even after the twofold averaging process.

The relative positions of the polypeptide chains of the CTP–enzyme complex were then manipulated to create a model of the PALA–enzyme complex. Each chain was treated as two separate domains, and then these domains were moved as separate rigid bodies. The catalytic chain was divided into a polar domain and an equatorial domain. The regulator chain was divided into a nucleotide-binding domain and a Zn domain.

The parameters of movement shown in Table 1 were examined independently. For each set of parameters, the atomic coordinates were altered, an electron density map was calculated, and the map was back transformed to obtain a set of amplitudes, which were compared with the measured amplitudes. The correlation coefficient between the observed amplitudes and the back-transformed amplitudes proved to be a far more sensitive guide than the conventional R factor in the evaluation of our many trial models. When parameters were far from their optimal values, the R factor varied only slightly. However, the correlation coefficient

$$\text{Corr} = \frac{\Sigma(F_o - \bar{F}_o)(F_c - \bar{F}_c)}{[\Sigma(F_o - \bar{F}_o)^2(F_c - \bar{F}_c)^2]^{1/2}}$$

proved to be a sensitive monitor of the optimization procedure, largely because it is independent of scaling problems between the F_os and the F_cs. The conventional R factor $R = \Sigma|F_o - F_c|/\Sigma F_o$, which requires scaled amplitudes, may be relatively insensitive because the scaling changes during the optimization procedure.

All of the final values for these parameters are shown in Table 1. The molecular model, which showed a clear molecular outline, was very different from the CTP–enzyme structure. This model was used to obtain initial phases.

The striking features of this model are the expansion along the threefold axis and the rotations of c_3s around the threefold axis and r_2s around the twofold axes. These movements preserve certain contact areas between r/c pairs and are quite consistent with the suggestion that c–r–r–c is an important functional unit (24, 25) (this suggestion does not diminish the importance of c–c interactions, particularly within a given c_3 unit). The c_3s are rotated a total of 9° relative to each other, so that they are in a more eclipsed configuration (Fig. 2*A*). The polar domain of

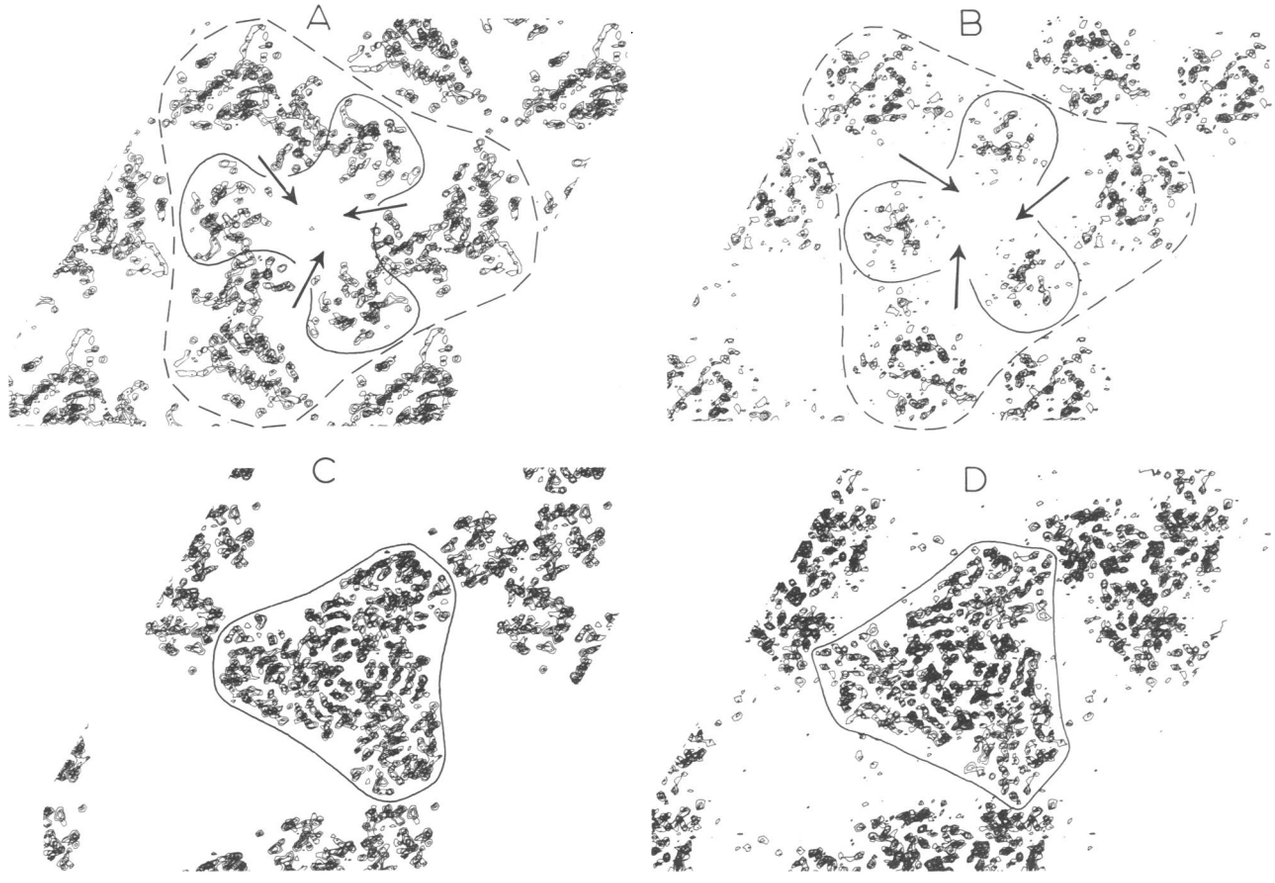

FIG. 3. Comparisons of the 10-Å slabs of electron density maps: (*A*) Central cavity area in the CTP–enzyme complex. The molecular outline is indicated by broken lines, the c_3 unit by a solid outline, and the access channels by arrows. (*B*) Central cavity area in the PALA–enzyme complex. (*C*) Top of c_3 in the CTP–enzyme complex, outlined by a solid line. (*D*) Top of c_3 in the PALA–enzyme complex. Because the lower c_3s (not shown here) are in coincidence in the CTP–enzyme crystals and the PALA–enzyme crystals, the entire relative rotation of 8–9° is visible when these upper c_3s are compared here in *C* and *D*.

each c is moved 6 Å away from the molecular center along z, a 12-Å molecular expansion. Each equatorial domain is moved 5 Å along z and 2 Å in x and rotated $-1.5°$ around the twofold axis. The r_2s are reoriented by 14–15° around the twofold axes, following the movements of the c_3s. The two Zn domains are moved 2 Å apart along z. The prominent effects of these movements are expansion of the central cavity and enlargement of the channels that allow access to the central cavity. In Fig. 2 we show the enlargement of the cavity as a view along the twofold axis, and in Fig. 3 we present a cross section of the electron density map that shows the effect of the expansion on the center portion of the molecule and also on the channels, which are indicated by arrows.

In some earlier experimental work, the PALA-induced elongation of the enzyme had been anticipated. The lengthening of the c axis of the PALA–enzyme crystals, compatible with a molecular expansion along c by about 8 Å, was noted by Monaco (21, 22). Ultracentrifugation experiments that demonstrated an increase in the frictional coefficient of the enzyme in the presence of PALA were interpreted in terms of a 3.5% expansion of a spherical model, or an expansion (or contraction) of an ellipsoid model (26). Moody *et al.* (27) predicted the 10- to 12-Å expansion from an analysis of PALA-induced structural changes, using the known structure of the T form of the enzyme and low-angle x-ray scattering data. However, the rotations of the subunits and domains were never correctly anticipated.

Our work was done with crystals grown at pH 5.8. At this pH the enzyme shows neither activity nor regulatory susceptibility. Our results, however, are in agreement with the solution studies mentioned above, which were performed at higher pH. Also, the evidence from mercurial-induced enzyme dissociation indicates that there are large differences between the unliganded enzyme and the PALA–enzyme complex at pH 6.0 (28). Further structural and biochemical studies of the pH dependence of the conformational changes are desirable.

Tertiary structural changes and the location of the PALA molecule will be discussed in a later publication.

We thank the National Cancer Institute for the gift of the PALA, and we acknowledge support from the National Institutes of Health, Grant GM06920.

1. Gerhart, J. C. & Pardee, A. B. (1962) *J. Biol. Chem.* **237**, 891–896.
2. Bethell, M. R., Smith, K. E., White, J. S. & Jones, M. E. (1968) *Proc. Natl. Acad. Sci. USA* **60**, 1442–1449.
3. Gerhart, J. C. & Pardee, A. B. (1964) *Fed. Proc. Fed. Am. Soc. Exp. Biol.* **23**, 727–735.
4. Monod, J., Wyman, J. & Changeux, J.-P. (1965) *J. Mol. Biol.* **12**, 88–118.
5. Weber, K. (1968) *Nature (London)* **218**, 1116–1119.
6. Wiley, D. C. & Lipscomb, W. N. (1968) *Nature (London)* **218**, 1119–1121.
7. Wiley, D. C., Evans, D. R., Warren, S. G., McMurray, C. H., Edwards, B. F. P., Franks, W. A. & Lipscomb, W. N. (1972) *Cold Spring Harbor Symp. Quant. Biol.* **36**, 285–290.
8. Honzatko, R. B., Crawford, J. L., Monaco, H. L., Ladner, J. E., Edwards, B. F. P., Evans, D. R., Warren, S. G., Wiley, D. C., Ladner, R. C. & Lipscomb, W. N., *J. Mol. Biol.*, in press.
9. Kantrowitz, E. R., Pastra-Landis, S. C. & Lipscomb, W. N. (1980) *Trends Biochem. Sci.* **5**, 124–128.
10. Kantrowitz, E. R., Pastra-Landis, S. C. & Lipscomb, W. N. (1980) *Trends Biochem. Sci.* **5**, 150–153.
11. Collins, K. D. & Stark, G. R. (1971) *J. Biol. Chem.* **246**, 6599–6605.
12. Howlett, G. J. & Schachman, H. K. (1977) *Biochemistry* **16**, 5077–5083.
13. Gerhart, J. C. & Holoubek, H. (1967) *J. Biol. Chem.* **242**, 2886–2892.
14. Crawford, J. L. (1977) Dissertation (Harvard Univ., Cambridge, MA).
15. Crowther, R. A. (1967) *Acta Crystallogr.* **22**, 758–764.
16. Crowther, R. A. (1969) *Acta Crystallogr. Sect. B* **25**, 2571–2580.
17. Ten Eyke, L. F. (1973) *Acta Crystallogr. Sect. A* **29**, 183–191.
18. Ten Eyke, L. F. (1977) *Acta Crystallogr. Sect. A* **33**, 486–492.
19. Bricogne, G. (1974) *Acta Crystallogr. Sect. A* **30**, 395–405.
20. Bricogne, G. (1976) *Acta Crystallogr. Sect. A* **32**, 832–847.
21. Monaco, H. L. (1978) Dissertation (Harvard Univ. Cambridge, MA).
22. Monaco, H. L., Crawford, J. L. & Lipscomb, W. N. (1978) *Proc. Natl. Acad. Sci. USA* **75**, 5276–5280.
23. Kuttner, P. G. (1980) Dissertation (Harvard Univ., Cambridge, MA).
24. Markus, G., McClintock, D. K. & Bussel, J. B. (1971) *J. Biol. Chem.* **246**, 762–771.
25. Chan, W. W.-C. (1975) *J. Biol. Chem.* **250**, 668–674.
26. Gerhart, J. C. & Schachman, H. K. (1968) *Biochemistry* **7**, 538–552.
27. Moody, M. F., Vachette, P. & Foote, A. M. (1979) *J. Mol. Biol.* **133**, 517–532.
28. Lauritzen, A. M. & Lipscomb, W. N. (1980) *Biochem. Biophys. Res. Commun.* **95**, 1425–1430.